Inorganica Chimica Acta 429 (2015) 114–121

Contents lists available at ScienceDirect

Inorganica Chimica Acta

journal homepage: www.elsevier.com/locate/ica

Investigation of a novel trinuclear μ-oxo ruthenium complex as a potential nitric oxide releaser for biological purposes

Natacha Cacita [a], Bruna Possato [a], Camila F.N. da Silva [a], Michele Paulo [b], André Luiz Barbosa Formiga [c], Lusiane M. Bendhack [b], Sofia Nikolaou [a,*]

[a] Departamento de Química, Faculdade de Filosofia Ciências e Letras de Ribeirão Preto da Universidade de São Paulo, Av. Bandeirantes, 3900, CEP 14040-901, Monte Alegre, Ribeirão Preto, SP, Brazil
[b] Faculdade de Ciências Farmacêuticas de Ribeirão Preto da Universidade de São Paulo, Av. do Café s/n°, CEP 14040-903, Monte Alegre, Ribeirão Preto, SP, Brazil
[c] Instituto de Química da Universidade Estadual de Campinas – UNICAMP, P.O. Box 6154, CEP 13083-970, Campinas, São Paulo, Brazil

ARTICLE INFO

Article history:
Received 2 September 2014
Received in revised form 18 December 2014
Accepted 26 January 2015
Available online 16 February 2015

Keywords:
Trinuclear ruthenium complex
Nitric oxide releaser
Photolysis
Vasorelaxing property

ABSTRACT

The chemical properties of the trinuclear ruthenium complex $[Ru_3O(CH_3COO)_6(3\text{-pic})_2(NO)]PF_6$ (**1**, were 3-pic = 3-picoline or 3-methylpyridine), its photochemical behavior and its ability as a vasorelaxing agent are reported in this work. It was shown that the unpaired electrons of NO and of the metal center $[Ru_3O]^+$ are tightly coupled, promoting an intermediate NMR profile between the oxidized (paramagnetic) and reduced (diamagnetic) $[Ru_3O]^{1+/0}$ species. From IR measurements, it was suggested that in trinuclear complexes, unlike other ruthenium compounds, the interaction of those unpaired electrons overcomes the effect of peripheral ligands and NO-backbonding on the ν(NO) frequency, which shows no dependence on the pK_a values of pyridinic ligands. The photoinduced NO release was investigated by light irradiation at 337, 447, 532 and 660 nm in phosphate buffer solution (pH 7.4), leading to the generation of gaseous NO^0 and the solvated species $[Ru_3O(CH_3COO)_6(3\text{-pic})_2(H_2O)]^+$ (**2**). Through amperometric and quimioluminescence measurements, the amount of NO(g) released were determined, showing dependence on the wavelength of irradiation. The ability of compound **1** as a vasorelaxing agent was also addressed. It was shown that, under ambient luminosity, compound **1** promotes 89% of relaxation in pre-contracted rat aorta. Molecular modeling of the novel nitrosyl, as well as characterization of the complexes $[Ru_3O(CH_3COO)_6(3\text{-pic})_2(L)]^n$, L = H_2O, n = +1 (**2**), L = 3-pic, n = +1 (**3**), L = CO, n = 0 (**4**), are also reported.

1. Introduction

In recent years, the possible applications of metal-nitrosyl compounds in biological systems as potential NO scavengers or releasers, has attracted much attention [1–6]. Light irradiation and electrochemical reduction of coordinated NO^+ are alternatives for the selective release of NO from coordination compounds. Both strategies take into account the low affinity of NO^0 by some metal centers [7].

Due to its similarities to iron, ruthenium is considered to have low toxicity, which in general is related to the available oxidation states. In this regard, ruthenium ions constitute an interesting alternative to iron, because it can achieve various oxidation states (II, III, IV) in physiological environment [8]. Also, its complexes have the ability to act both as NO scavengers or releasers, increasing the interest on the development of a variety of nitrosyl ruthenium complexes [5,8–16].

Also of interest to this work, the trinuclear complexes of general formula $[M_3O(CH_3COO)_6(L)_3]^n$ (M = transition metal, L = solvent or N-heterocyclic ligands) are part of an important class of compounds of transition metals [17–22]. These complexes have a triangular structure in which the metal ions are held together by a μ-oxo and carboxylate bridges (Fig. 1) [19,23]. In such compounds, the proximity of the ruthenium atoms leads to a strong metal–metal interaction, both magnetic and electronic, enhancing the electron delocalization over the $[Ru_3O]^+$ core, which behaves like a single metal center [24]. Besides the rich redox, electrochromic and catalytic properties, species containing labile and/or bridging ligands can act as building blocks to assemble supramolecular structures [18,19,24–28]. The $[Ru_3O(CH_3COO)_6)]$ moiety also appears as an appealing unit to react with NO^0. It has been shown that the strong interaction between the unpaired electrons of NO and $[Ru_3^{III,III,III}O]$ unit accounts for interesting properties [9,10].

* Corresponding author.
E-mail address: sofia@ffclrp.usp.br (S. Nikolaou).

http://dx.doi.org/10.1016/j.ica.2015.01.038
0020-1693/

Recently, our group reported the very first example of a trinuclear ruthenium complex which acts against cancer cells [29]. Complex $[Ru_3O(CH_3COO)_6(4\text{-pic})(NO)]PF_6$ lowers up to 90% the viability of B16F10 melanoma cell when irradiated with visible light (532 nm). It also presented some dark activity, which works in synergism with NO release triggered by light, potentiating the compound biological activity.

In this context, this work presents the synthesis and characterization of the novel complex $[Ru_3O(CH_3COO)_6(3\text{-pic})(NO)]PF_6$ (**1**), where 3-pic = 3-methylpyridine, Fig. 1. Although $[Ru_3O]$ complexes have been extensively studied, there are very few examples of this sort of compounds coordinated to NO. In this context, one of our aims is to introduce in literature a new set of characterization data in order to expand the number of described $[Ru_3O]$-nitrosyls monomeric units. Besides that, the presence of methyl groups provides some hydrophobicity to the whole system, an important aspect to be addressed for biological applications. We also intend to advance on the investigation of photoinduced NO release by verifying the ability of **1** to delivery NO in physiological like medium under irradiation with visible light. Finally, we present its vasorelaxing capacity, probed by relaxation of pre-contracted rat aorta. Characterization of the precursors $[Ru_3O(CH_3COO)_6(3\text{-pic})(L)]^n$, L = H_2O, n = +1 (**2**), L = 3-pic, n = +1 (**3**), L = CO, n = 0 (**4**), is also reported.

2. Results and discussion

2.1. Electronic spectroscopy, molecular modeling and electrochemical measurements

The data collected from the absorption spectra of compounds **1**–**4** are reported in Table 1. Compounds **2**–**4** behaves as expected, following the well described characteristics of the trinuclear ruthenium clusters [17,19]. More relevant to this discussion are the features of compound **1**.

The electronic spectrum of the complex $[Ru_3O(CH_3COO)_6(3\text{-pic})_2(NO)]PF_6$ is shown in Fig. 2, being consistent with the profile observed earlier for trinuclear ruthenium complexes coordinated to nitric oxide [9,10]. The classical description of the electronic structure of a trinuclear ruthenium complex has been done on a qualitatively basis, in terms of the molecular orbital diagram proposed by Cotton and Norman [30]. This diagram addresses the $[Ru_3O]$ π system under D_{3h} symmetry for complexes of general formula $[Ru_3O(CH_3COO)_6(L)_3]^n$, and C_{2v} for asymmetric complexes, such as compound **1**. The central oxygen atom is considered to have sp^2 hybridization, leaving a p_z orbital of π symmetry free to interact with the ruthenium dπ orbitals [17,30]. Following this description, the electronic spectra of trinuclear ruthenium complexes of +1 charge (a Ru_3(III)(III)(III)O unit) are dominated by cluster-to-ligand charge transfer bands (CLCT) in the UV and visible region (below 500 nm), and a strong low-energy broad band named intra-cluster (IC), around 700 nm, in which a metallic character predominates [17–19,23,31,32].

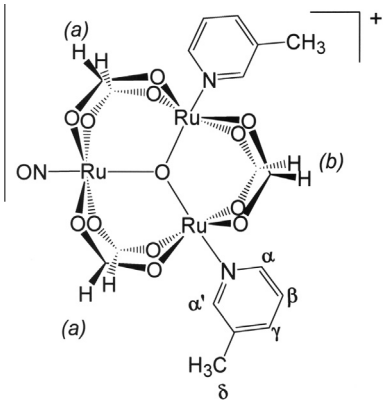

Fig. 1. Structure of $[Ru_3O(CH_3COO)_6(3\text{-pic})_2(NO)]PF_6$, and labeling for ^1H NMR assignment.

Table 1
Absorption and electrochemical data for compounds **1**–**4** collected from acetonitrile solutions.

Electronic spectra data	λ_{max} (nm)/log ε (mol^{-1} L cm^{-1})			
	IC	CLCT	CLCT	CLCT
$[Ru_3O(CH_3COO)_6(3\text{-pic})_2(NO)]^+$(**1**)	709/ 2.86*	542/ 3.21	456/ 3.28	372/ 3.39
Molecular modeling prediction for (**1**)	753	521	460	372
$[Ru_3O(CH_3COO)_6(3\text{-pic})_2(H_2O)]^+$(**2**)	679/ 3.45			312/ 3.76
$[Ru_3O(CH_3COO)_6(3\text{-pic})_3]^+$ (**3**)	688/ 3.73			313/ 4.05
$[Ru_3O(CH_3COO)_6(3\text{-pic})_2(CO)]$ (**4**)	587/ 3.51			327/ 3.75
Electrochemical data	$E_{1/2}$ (V vs. Ag/AgCl)			
	$[Ru_3O]^{-1/0}$	$[Ru_3O]^{0/1+}$	$[Ru_3O]^{1+/2+}$	
$[Ru_3O(CH_3COO)_6(3\text{-pic})_2(NO)]^+$(**1**)	−0.77	−0.06	1.38	
$[Ru_3O(CH_3COO)_6(3\text{-pic})_2(H_2O)]^+$(**2**)	−1.21	0.039	1.04	
$[Ru_3O(CH_3COO)_6(3\text{-pic})_3]^+$ (**3**)	−1.31	−0.049	0.98	
$[Ru_3O(CH_3COO)_6(3\text{-pic})_2(CO)]$ (**4**)	−0.85	0.65	1.27	

* In the case of compound **1**, the intra-cluster band has contribution of NO levels, having some character of charge transfer as well.

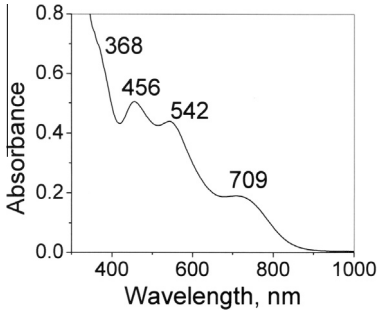

Fig. 2. Electronic spectrum of complex $[Ru_3O(CH_3COO)_6(3\text{-pic})_2(NO)]PF_6$, collected from a 10^{-3} M acetonitrile solution.

Although this description has worked well for a very large number of compounds [19], it seems to fail to describe the profile observed in Fig. 2. It is well known that for reduced ($[Ru_3O]^0$) compounds, both CLCT and IC transitions experience a large bathochromic shift, the last one moving further than 900 nm [19]. The coordination of a strong π-acceptor ligand such a CO to a reduced $[Ru_3O]^0$ core promotes a noticeable hypsochromic shift of the IC band, which usually lays below 600 nm [18,19,33,34]. NO^+ has a stronger π-acceptor character than CO, although for NO^0 the effect of π-backbonding is attenuated by the presence of the unpaired π-electron, allowing the formation of a stable complex with the oxidized $[Ru_3O]^+$ unit, such as compound **1** [9,20,35]. Indeed, Zhou et al. have discussed on this matter in their work [35]. They have shown the possibility to exchange a CO by a NO ligand in the structure of a trinuclear ruthenium compound by electrochemical control of the charge of the $[Ru_3O]$ unit. The oxidation of a CO-$[Ru_3O]^0$ cluster to the CO-$[Ru_3O]^+$ species in the presence of NO leads to ligand substitution, with formation of the stable NO-$[Ru_3O]^+$ moiety.

The spectrum displayed in Fig. 2 is not entirely compatible neither with a $[Ru_3O]^{1+}$ nor with a $[Ru_3O]^0$ core, since it displays

Table 2
ν(NO) values for complexes $[Ru_3O(CH_3COO)_6(L)_2(NO)]^+$, and p$K_a$ values of ligands L.

L	ν(NO) (cm^{-1})	pK_a	Refs.
4-Acpy	1874	3.51	unpublished data
Py	1865	5.25	[9]
3-Pic	1883	5.63	this work
4-Pic	1874	5.98	[10]

4-Pic = 4-methylpyridine; 4-acpy = 4-acethylpyridina.

absorption bands within all visible region (400–800 nm), and no other absorptions up to 1100 nm. In previous works, Toma et al. made the calculations of the molecular orbital diagram for the complexes $[Ru_3O(CH_3COO)_6(L)_2(NO)]^+$, where L = pyridine or 4-methylpyridine, showing that the NO contribution on different energy levels of the cluster is rather high, particularly to those levels involving the dxz and dyz orbital of the ruthenium ions [9,10]. In this context, the usual spectra assignment in terms of CLCT and IC does not strictly apply, since the NO-$[Ru_3O]$ orbital mixing is high, even for the levels where metallic character predominates.

In our case, it is reasonable to assume a parallelism of the spectroscopic behavior of **1** with that of compound $[Ru_3O(CH_3COO)_6(4\text{-pic})_2(NO)]^+$, (4-pic = 4-methylpyridine) [10], since the ligand 3-pic is a position isomer of ligand 4-pic and presumably will not introduce a strong perturbation on the electronic structure of compound **1**.

This is actually seen in the semiempirical theoretical study of **1**, performed by a combination of PM3(tm) and ZINDO/S investigation (the optimized structure of **1** and the relative contributions of the $[Ru_3O]$ and NO orbitals on compound **1** levels are available as Supporting information). As one can see in Table 1, the theoretical and experimental transitions are in good agreement. The geometry obtained with PM3(tm) for compound **1** is equivalent to the reported earlier, and for all complexes the final structure is composed of a planar isosceles Ru_3O triangle with two equivalent Ru-μ_3O bonds of 1.905 Å and a longer one (2.005 Å) *trans* to NO. The nitrosyl is linearly coordinated to the trinuclear cluster and also the NO distance is essentially the same for both complexes (1.145 Å). All these structural parameters are in accordance with experimental geometries for related complexes [19]. The elongation of the Ru-μ_3O bond *trans* to NO can be related to a strong interaction between this non-innocent ligand and the ruthenium ion resulting in an antiferromagnetic coupling of the unpaired electrons on Ru_3O and NO and a consequent singlet ground state. ZINDO/S calculations also revealed the same theoretical spectral profile as reported before, the only difference being the shift of the transitions, which are red-shifted in the order: pyridine ~ 3-picoline < 4-picoline. Mulliken population analysis based on the ZINDO/S wavefunctions revealed that the charge on NO is essentially zero (0.02) for the complex, corroborating with the previous NO^0 assignment for this class of cluster in the $Ru_3^{III}O$ oxidation state.

Although Mulliken population analysis is known to be basis set dependent and should be used with caution, these qualitative results are indicative that the electronic coupling between NO and the metal center can explain the linear NO coordination mode to Ru_3O, even if NO is still regarded as a formal zero charge ligand. Indeed, Ford and co-workers have recently shown that NO can coexist as linear and bent coordination isomers depending on the spin state of a MnII(NO)porphyrinate complex [36]. They have found that singlet ground state is linearly coordinated but for another very close triplet state NO is bent with essentially the same configuration for Mn(II), i.e., the formal oxidation states of the metal center and NO are not changed. Therefore, even considering the present semiempirical calculations from a qualitative viewpoint, our results are indicative that such a behavior cannot be ruled out for compound **1**.

Regarding the electrochemical behavior of compounds **1**–**4**, the data collected from cyclic voltammetry measurements are depicted in Table 1. All compounds display three waves attributed to the successive redox couples $Ru^{III}Ru^{II}Ru^{II}/Ru^{III}Ru^{III}Ru^{II}/Ru^{III}Ru^{III}Ru^{III}/Ru^{III}Ru^{III}Ru^{IV}$. The electrochemical behavior is quasi-reversible, showing current ratios close to 1, and about 70 mV for the anodic/cathodic peak separation. The behavior is fully consistent with that reported for analogous compounds [9,10,19].

Worth mentioning is the fact that for compounds **1** and **4** (nitrosyl and carbonyl clusters, respectively) the difference between successive $E_{1/2}$ values is not as regular as for the pyridinic complexes [19]. In the case of the carbonyl cluster **4**, the strong π-backbonding between CO and $[Ru_3O]$ unit stabilizes the reduced form of the latter, shifting the $E_{1/2}$ value of the process $[Ru_3O]^{0/1+}$ to more positive values. One could expect the same behavior for the nitrosyl cluster **1**, however the presence of the unpaired electron on ligand NO^0 and its strong coupling with the unpaired electron of the $[Ru_3O]^{1+}$ seems to favor the formation of the +1 species, shifting the $E_{1/2}$ value of the process $[Ru_3O]^{0/1+}$ to more negative values. These observations corroborate the analysis made from UV–Vis spectroscopy.

2.2. Infrared spectroscopy

The infrared spectra of complexes **1**–**4** were assigned by comparison to similar complexes previously reported in the literature [9,10,19] (Supplementary information). The NO stretching was observed at ν(NO) = 1883 cm^{-1}. This peak is quite symmetrical and is not observed in the precursor $[Ru_3O(CH_3COO)_6(3\text{-pic})_2(H_2O)]PF_6$. The value occurs within the typical range for nitrosyl complexes with a linear M-NO coordination, close to the vibrational frequency of free NO (1876 cm^{-1}) [44]. The remaining peaks are associated with the vibration characteristics of the acetate, the picoline and the PF_6^- species.

Aiming to address the effect of co-ligands in the infrared spectra of trinuclear ruthenium nitrosyls, Table 2 presents the values of ν(NO) frequencies for few different complexes of general formula $[Ru_3O(CH_3COO)_6(L)_2(NO)]^+$, where L are pyridinic ligands with different pK_a. Nitric oxide coordinated to ruthenium ions generally has an intense band in the range of 1800–1970 cm^{-1}, which frequency depends on the metal oxidation state and the stereochemistry of the NO bond with the ion [1,37,38]. It is also known that, typically, several classes of ruthenium nitrosyl show a correlation between the value of ν(NO) and the pK_a value of the respective co-ligands. This correlation reflects the weakening of the nitrogen–oxygen bond of NO due to the strengthening of π-backbonding with the metal center which, in turn, is influenced by the pK_a of other ligands [39–42].

In the case of the trinuclear ruthenium complex this typical behavior does not seem to manifest. It is observed that even for ligands with very different pK_a values such as 4-acethylpyridine and 4-methylpyridine, the values of ν(NO) do not suffer significant displacements, as well as do not show any clear trend of dependence on co-ligand pK_a. Possibly this finding corroborates the fact that, in the case of trinuclear ruthenium complexes the behavior of the metal center and the NO ligand is more dependent on the strong interaction between the two units (through orbital mixing and interaction between their unpaired electrons) than on the influence of peripheral ligands L. However it is important to note that this is a preliminary analysis, since the series of ligands L exploited so far is still small [9,10, thiswork].

2.3. ^1H NMR and EPR

The ^1H NMR spectra of compounds **1**–**4** were assigned by comparison with analogous complexes [9,10], with the free ligands and

from the correlations observed on COSY spectra (Supplementary information). The NMR spectra are available as Supplementary material, and the relevant data for our discussion are reported in Table 3.

It is well described that the signals of ligands coordinated to the $[Ru_3O]$ moiety are dependent on the oxidation state of the ruthenium ions. Reduced complexes ($[Ru_3O]^0$) having the formal oxidation states $Ru^{III}Ru^{III}Ru^{II}$ are diamagnetic and the signals of coordinated ligands are near to the chemical shift values observed for the corresponding free ligands [34,43–45]. On the other hand, $[Ru_3O]^{1+}$ complexes (formal oxidation states $Ru^{III}Ru^{III}Ru^{III}$) have one unpaired electron, being paramagnetic. Therefore, the signals of their ligands are not only sensitive to inductive effects, but also to the paramagnetism of the $[Ru_3O]$ unit [19,45,46]. The effect of paramagnetic anisotropy can manifest itself in two different ways: by the pseudocontact mechanism, which involves a through space dipole interaction, decreasing with the distance. And/or the contact mechanism, that depends on the orientation of a nucleus in relation to the paramagnetic center. The latter promotes shifts either to higher or lower fields [46]. Typically, for an oxidized cluster such as precursor **2**, the protons at α position of the pyridinic ligand shifts to higher field in relation to free ligand and the CH_3 groups of the acetates exhibit shifts to lower field (Table 3). The shifts on the pyridinic hydrogen signals decrease with distance, being consistent with the pseudocontact mechanism of paramagnetic interaction (Table 3). This typical behavior expresses the paramagnetic effect on the unit $[Ru_3O]^{1+}$.

Nevertheless, one can observe in Table 3 that the chemical shift values observed for the hydrogen nucleus of the nitrosyl **1**, a paramagnetic complex at principle, are somewhat different from the values observed for compound **2**. In fact, compound **1** displays intermediate values of chemical shift between the values observed for the free ligands (diamagnetic species) and the values observed for oxidized clusters (paramagnetic species). This result confirms that the interaction of the unpaired electrons of the $[Ru_3O]^{1+}$ and the NO^0 ligand is so severe that partially removes the paramagnetic anisotropy effect, promoting in complex **1** an intermediary behavior between that of paramagnetic (**2**) and diamagnetic (free ligands) species.

Actually, the EPR spectra of compound **1**, both in solid state and in acetonitrile solution, are silent, displaying no signals (Supporting information). This means that compound **1**, despite of having two unpaired electrons, is a diamagnetic species, supporting the hypothesis of having antiferromagnetic coupling between the $[Ru_3O]^{+1}$ center and NO^0 ligand.

2.4. Photolysis

Photolysis of the nitrosyl **1** were performed in phosphate buffer, pH 7.4, to simulate physiological environment and spectra changes were monitored as a function of time for different irradiation wavelengths (377 nm, 447 nm and 660 nm, Supplementary information). Fig. 3 presents the result for irradiation at 532 nm.

Table 3
Data obtained from ^1H NMR analysis for compounds $[Ru_3O(CH_3COO)_6(3\text{-pic})_2L]PF_6$ (L = NO and H_2O, **1** and **2**, respectively), from acetonitrile-d_3 solutions.

δ (ppm)	1	2	3-Pic[a]	Acetate[a]
CH_3(a)	3.93 (12H)	4.73 (12H)	–	2.1
CH_3(b)	3.25 (6H)	4.83 (6H)	–	2.1
Hα	4.32 (2H)	−1.65 (2H)	8.42	–
Hα′	4.28 (2H)	−1.65 (2H)	8.44	–
Hβ	8.04 (2H)	−1.49 (2H)	7.16	–
Hγ	5.51 (2H)	5.85 (2H)	7.45	–
Hδ	1.78 (6H)	5.88 (6H)	2.32	–

[a] ^{13}C and ^1H NMR collection from Aldrich.

Regarding the spectra profile changes, the behavior of **1** during irradiation at 377, 447 and 532 nm is the same, showing a gradual decrease in the 452 nm band, a bathochromic shift of the 542 nm transition and the formation of a band at 680 nm, generating a spectrum profile for the photoproduct that is fully compatible with the spectrum of precursor **2**, $[Ru_3O(CH_3COO)_6(3\text{-pic})_2(H_2O)]^+$. Isosbestic points around 400 nm and 550 nm, with slight variations for each irradiation wavelength were observed, indicating that the reaction that occurs during photolysis is the same for all λ_{irrad}. From the spectroscopic investigation, apparently NO cannot be released by irradiation within the therapeutic window (λ_{irrad} = 660 nm), what would be more interesting for bioinorganic purposes.

In order to accomplish the specific detection of NO, photolysis was performed with irradiation at the same wavelengths, 377, 447, 532 and 660 nm, but using a selective electrode for $NO_{(g)}$ detection at this time. The chronoamperograms corresponding to this photolysis are presented in Fig. 4.

Immediately after exposing the solution to laser irradiation, the chronoamperogram indicated substantial increase in current detected by the selective electrode, indicating the photochemical production of $NO_{(g)}$. We estimated the amount of $NO_{(g)}$ released by the photoinduced reaction, using an analytical curve (available as Supplementary information), and the values are shown in Table 4.

It is observed that at wavelengths lower than 450 nm, NO release is higher. Furthermore, NO release is still photoinduced in visible region (532 nm), although with a much lower efficiency. Again, we failed to detect NO within the sensitivity of the amperometric experiment using 660 nm as irradiation wavelength.

These observations could easily be rationalized in terms of the selective irradiation of charge-transfer transitions (region addressed by the 377, 447 and 532 nm) and irradiation of a transition of metallic character (660 nm), particularly because it is the typical behavior observed for other ruthenium nitrosyls, which generally deliveries NO from irradiation of the CT excited states [47]. However, this argument should not entirely apply to compound **1**, taking into account the high orbital mixing between NO and the metallic unit proposed from the molecular modeling results, which is consistent with the other data reported in this work. The orbital mixture occurs with a greater extent in the ultraviolet region, but also is considered to be relevant for the lower energy levels [9,10,thiswork].

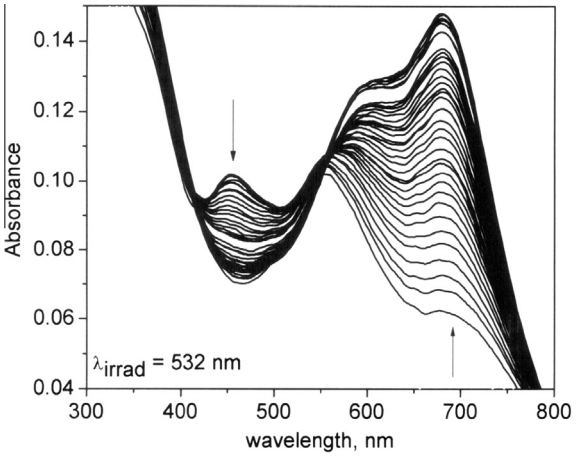

Fig. 3. Electronic spectra of the complex $[Ru_3O(CH_3COO)_6(3\text{-pic})_2(NO)]PF_6$ (5.5×10^{-5} M, pH 7.4) in phosphate buffer solution during photolysis with irradiation at 532 nm.

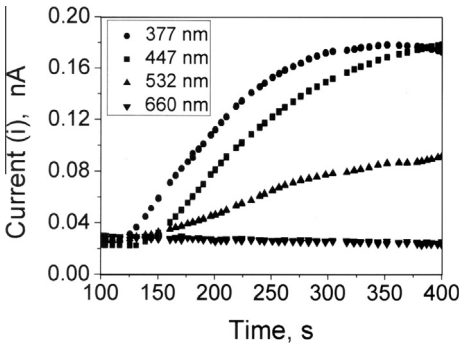

Fig. 4. Cronoamperogram of NO release in phosphate buffer, pH 7.4.

Therefore, we further tried to detect NO release by stimulation with λ_{irrad} = 660 nm performing a NOA experiment (Nitric Oxide Analyzer), which detects $NO_{(g)}$ under a helium flow, pushing the experiment limits of sensitivity to the range of 1 picomolar to μM concentrations [48]. It was also verified the $NO_{(g)}$ release in the presence of ascorbic acid, to simulate the reaction with endogenous reducing agents. The results are shown in Fig. 5.

It is seen that compound **1** in fact deliveries NO as a consequence of irradiation within the therapeutic window, although with less efficiency than when irradiated with higher energy light. It is also observed that the release is much more pronounced in the presence of a reducing agent such as ascorbic acid. This fact is not surprising, since it has been recently described the release of NO from the analog $[Ru_3O(CH_3COO)_6(4\text{-pic})_2NO]PF_6$, triggered by a redox reaction with ascorbic acid [29].

In compound (**1**), formally the $[Ru_3O]$ unit presents +1 formal charge, while coordinated NO is neutral. One possibility to explain the release of NO mediated by ascorbic acid, is that the reductant acts on the metallic unit, not on the ligand. The implication here is that lowering the oxidation state of the metal center decreases the affinity with the coordinated NO^0 as much as reducting a coordinated nitrosonium ion decreases the affinity with a metal center of lower oxidation states.

However, the reactivity of $[Ru_3O]$ compounds with ascorbic acid might be more complicated. Recently it was reported the reactivity of the analog $[Ru_3O(CH_3COO)_6(H_2O)_3]^+$ with ascorbic acid at pH 3.8 (acetate buffer) [49]. The authors have shown that the first reaction step occurs with the selective reduction of one Ru(III) ion concomitantly with the cleavage of one acetate bridge. This leads to the formation of aquo/hydroxo species. After that, further reduction reactions take place with decomposition of the $[Ru_3O]$ unit.

We have performed a qualitative evaluation of the interaction between **1** and ascorbic acid, aiming to simulate the excess of ascorbic acid present in the experimental conditions of the NOA-nalyser experiment. Thus, a 2 M solution of ascorbic acid was prepared in phosphate buffer, and a 100 μL aliquot was added to 3 mL of a 0.2 mM complex solution (2% of DMSO, phosphate buffer), giving a proportion of 0.2 mmol of reductant to 0.6 μmol of complex. As a result, very little modification on the spectrum profile of **1** was observed after reaction with ascorbic acid (spectra available as Supporting information). Besides that, the final spectrum does not match the profile observed either for the species described by Dasgupta et al. [49], or for the reducted nitrosilated analog $[Ru_3O(CH_3COO)_6(4\text{-pic})_2NO]^0$, generated electrochemically [10]. In our case, despite the fact that the spectra changes very little, one can observe the onset of an absorption in between 800 and 1000 nm, characteristic of solvated species $[Ru_3O(CH_3COO)_6(L)_2S]^0$. Therefore, in this particular case most probably it is occurring a reduction reaction centered on the metal unit $[Ru_3O]$, leading to release of the previously coordinated NO^0.

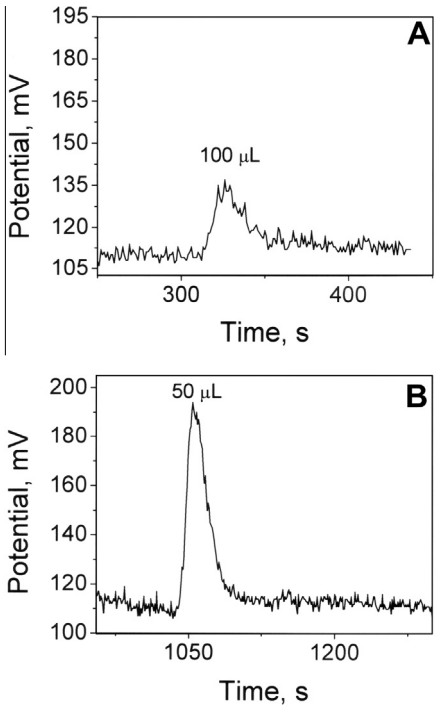

Fig. 5. NO release detected by NOA from a $[Ru_3O(CH_3COO)_6(3\text{-pic})_2(NO)]PF_6$ solution (5.89×10^{-5} M, phosphate buffer, pH 7.4) (A) irradiated at 660 nm; (B): in absence of light after reaction with a 45 mM solution of ascorbic acid.

Even though we have calculated the amount of NO released from different experiments (Table 4), it is possible to propose a qualitative discussion of the dependence of these values with the wavelength of irradiation. From the spectroscopic analysis, one can verify that all the transitions irradiated with the wavelengths used in photolysis experiments imply in molecular orbitals with different extents of NO character [9,10, thiswork]. However, it does not display an obvious correlation with the observed yields presented in Table 4, since orbital mixing is high. On the other hand, it is described that the $[Ru_3O]^{1+}$ unit constitute an excellent final acceptor of excitation energy in different polynuclear systems, mostly because it performs rapid photoinduced electron transfer reactions [50–52]. Also its decay is very fast, since the low lying energy levels associated with the IC transitions promotes a very rapid path for vibrational decay. In our case, presumably these low lying energy levels must quench the excited state responsible for NO release, due to the fast vibrational decay, leading to the observed lower value of delivered NO when irradiation takes place

Table 4
Quantum yields and amount of $NO_{(g)}$ released (mol/L) from compound $[Ru_3O(CH_3COO)_6(3\text{-pic})_2NO]PF_6$ in phosphate buffer solution (pH 7.4) for different irradiation wavelengths.

λ_{irrad} (nm)	ϕ	[NO][b] (10^{-6} M)	[NO][c] (10^{-12} M)
377	0.10	2.15	–
447	0.006	2.10	–
532	0.004	0.95	–
660	[a]	–	19
–	–	–	144[d]

[a] Quantum yields were not calculated for λ_{irrad} = 660 nm because there were not observable changes in the spectral profile of (**1**) during irradiation at this wavelength.
[b] Obtained from the chronoamperograms.
[c] Obtained by NOA.
[d] In the presence of the reducing agent ascorbic acid, [ascorbic acid] = 45 mM, PBS solution 0.01 M.

at 660 nm. Time-resolved measurements are under way in our laboratories, in order to properly describe this assumption.

Finally, values of quantum yields follow the same trend of the amount of NO released obtained using the NOmeter and NOA. Namely, for minor amounts of NO released, the quantum yield was also lower, depending on the irradiation wavelength (Table 4). If there was a significant rate of recombination, the observed dependence of amount of NO released on λ_{irrad} would not follow the same trend of quantum yields.

2.5. Preliminary essay on the vasorelaxing properties of compound **1**

Nitrosyl ruthenium compounds have already been studied as NO donor that induces rat aorta relaxation [53–56]. Taking it into account, we also evaluate the induced vasodilatation by $[Ru_3O(CH_3COO)_6(3\text{-pic})_2(NO)]^+$ in rat aortic rings pre-contracted with phenylephrin, which is a reducing agent.

As shown in Fig. 6(A), the relaxation induced by this compound in the presence of visible light (ambient light, the system set in a glass vessel) was concentration-dependent in denuded rat aortas pre-contracted with phenylephrine. The absence of light significantly reduced the relaxation induced by complex **1**: the ME (maximal effect) induced by the complex in the presence of visible light (89.9 ± 4.1%) was greater than ME induced by the complex in the absence of visible light (25.25 ± 2.24%), Fig. 6(B).

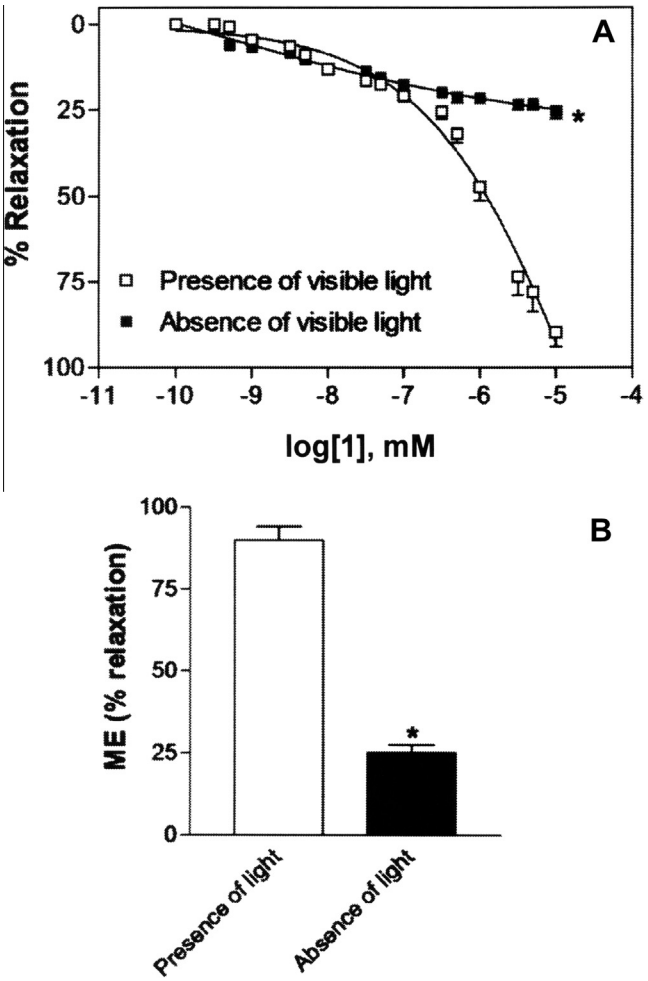

Fig. 6. (A) Effect of $[Ru_3O(CH_3COO)_6(3\text{-pic})_2(NO)]PF_6$ on rat thoracic aorta pre-contracted with phenylephrine 0.1 M in the presence and absence of visible light. (B) Maximum effect (ME) induced by $[Ru_3O(CH_3COO)_6(3\text{-pic})_2(NO)]$ PF_6 in aorta rings. Data are means ± SEM of experiments performed on 4 preparations obtained from different animals. $^*P < 0.05$.

This preliminary result leads us to two important conclusions. First, although the liberation of NO seems to occur mediated by a reduction reaction as well (presumably by phenylephrin), light plays an important role to maximize the effect of vasodilatation. Secondly, even with the apparent low yields of NO release (Table 4), compound **1** is still able to perform vasorelaxation with high efficiency, by stimulation with visible light.

3. Conclusions

This work presented the synthesis and characterization of the novel nitrosyl $[Ru_3O(CH_3COO)_6(3\text{-pic})_2(NO)]PF_6$ and of compounds **2**–**4** as well. Particularly the ^1H NMR measurements showed that complex (**1**) displays an average behavior between a reduced and an oxidized trinuclear complex. This reflects the significant increase in electron density of the $[Ru_3O]^{1+}$ unit, due to the extensive orbital mixing of the metallic and NO^0 levels and the consequent interaction between their unpaired electrons. The mixing also impacts the ν(NO) frequency observed in the infrared spectrum, which does not display the typical correlation with the co-ligands pK_a. The hypothesis of having the pairing of electrons is corroborated by a silent EPR result.

The photolysis results showed that compound **1** is able to release NO in physiological pH by irradiation with visible light and, more interesting, within the therapeutic window (660 nm). Its ability to induce vasodilatation was also probed both under ambient light and in the absence of light, under a reducing environment. Our results demonstrated that under ambient light the compound induced more than three times the rate of relaxation than in the absence of light. However, the dark activity reveals the possibility of using this kind of compound in therapies other than those mediated by light-induction.

Overall, our results show that compound **1** is a suitable candidate for the development of novel pro-drugs based on the $[Ru_3O(CH_3COO)_6]$ moiety, both as a carrier and a controlled NO releaser.

4. Experimental

The synthesis of precursors $[Ru_3O(CH_3COO)_6(3\text{-pic})_2(H_2O)]PF_6$, $[Ru_3O(CH_3COO)_6(3\text{-pic})_3]PF_6$ and $[Ru_3O(CH_3COO)_6(3\text{-pic})_2(CO)]$ were performed as previously described in the literature [17,19,57]. Complex $[Ru_3O(CH_3COO)_6(3\text{-pic})_2(H_2O)]PF_6$ was purified in a neutral alumina column, eluted with a mixture of 70% CH_3CN:30% CH_3OH. ESI-HRMS: $[\mathbf{2}-H_2O-PF_6]^+$ m/z 860,9; $[\mathbf{3}-PF_6]^+$ m/z 953,9 and $[\mathbf{4}+H^+]^+$ m/z 889.9.

4.1. Synthesis of $[Ru_3O(CH_3COO)_6(3\text{-pic})_2(NO)]PF_6$

A solution of dichloromethane, 33 mL, containing 0.35 g of $[Ru_3O(CH_3COO)_6(3\text{-pic})_2(H_2O)]PF_6$ complex was degassed with argon for 20 minutes, then it was bubbled NO for 2 h (generated by the reaction of nitric acid and copper pads, bubbled through a concentrated solution of NaOH to remove traces of NO_2), and again deaerated with Ar for 20 min. The product was precipitated by adding petroleum ether. The purple solid was collected on a filter, washed with petroleum ether and dried under vacuum in a desiccator with silica gel. Yield: 92 %. Elemental analysis: C, 27.8; H, 3.1; N, 4.1. Found: C, 26.5; H, 3.4; N, 5.1. ESI-HRMS: $[\mathbf{1} - PF_6]^+$ m/z 890,9.

4.2. Physical measurements

Infrared spectra were obtained from samples dispersed in KBr pellets in the region 400–4000 cm^{-1} with resolution of 4 cm^{-1} in an IR spectrophotometer Shimadzu Prestige 21. ^1H NMR and COSY

spectra were recorded on a Bruker Avance DRX- 500 500 MHz; from 1×10^{-2} M of the complexes in acetonitrile-d_3. High resolution mass spectra (HRMS) were collected in positive mode on a micrOTOF II-ESI-TOF Mass Spectrometer, with a flow rate of 300 μL pump/h, mobile phase MeOH:H_2O 1v:1v. EPR spectra were recorded in a Bruker EMX instrument operating at X-band (9.48 GHz frequency, 20 mW power, 100 kHz modulation frequency, 5–15 G modulation amplitude), at 77 K, in solid state and in acetonitrile solution, using Wilmad quartz tubes.

Electronic spectra were recorded on an Agilent 8453 spectrophotometer, in the region 190–1100 nm, using quartz cuvettes with optical path length of 1 cm. The cyclic voltammetry experiments were performed in a conventional three electrodes cell (platinum as working electrode; platinum wire as auxiliary electrode and Ag/AgCl as reference electrode; the reported $E_{1/2}$ values are uncorrected for junction potential values). A 0.1 M acetonitrile solution of tetrabutylammonium hexafluorophosphate ($TBAPF_6$) was prepared in 0.1 mol L^{-1} acetonitrile. The complexes solutions were prepared to have final concentrations around 1×10^{-3} M.

The photolysis of the $[Ru_3O(CH_3COO)_6(3\text{-pic})_2(NO)]PF_6$ complex was performed from 5.5×10^{-5} M solutions in aqueous phosphate buffer solution, pH 7.4. Since complex **1** is not fully soluble in water, a stock solution was prepared in the acetonitrile (5.5×10^{-3} Mol L^{-1}) and 30 μL aliquots were added to 2970 μL of buffer solution in quartz cuvette of 1 cm optical path, with a suitable magnetic stirrer. The solutions were stirred continuously during the irradiation time intervals (2 min) at different wavelengths (377, 447, 532 and 660 nm). The irradiation was performed with a laser tag Colibri Quantum Laser Tech. Three types of analyzes were performed during the photolysis experiments: first, the absorption spectra of the samples were recorded after each irradiation period until the original spectrum converges to the spectra of the solvated species **2**. Light intensities were determined by chemical actinometry (ferrioxalate and Reinecke salts) in order to calculate quantum yields.

The second experiment was performed using a selective electrode for $NO_{(g)}$ positioned inside the cuvette, but outside the light beam way, in order to avoid any photoelectric interference. The detection of NO was taken using this selective electrode for NO Noxímetro Brand Insight. NOmeter calibration was done monitoring the amount of dissolved $NO_{(g)}$ in a standard solution of NO gas [58]. This solution was prepared by bubbling NO for 1 h, to ensure saturation of 8 mL of phosphate buffer solution (pH 7.4) previously degassed to remove oxygen. The nitric oxide was generated from a solution of 50% nitric acid and metallic copper. Before bubbling through the buffer solution, the generated gas passed through a concentrated solution of NaOH to remove traces of NO_2. The concentration of NO of the final saturated solution is 2×10^{-3} M [59]. The analytical curve (Supporting information) was obtained by varying the concentration of NO adding known aliquots of the saturated solution to 6 mL of previously degassed phosphate buffer solution, pH 7.4, and monitoring the corresponding current value.

The third experiment was performed using a NOA 280i Nitric Oxide Analyzer. A 5.89×10^{-5} M solution of $[Ru_3O(CH_3COO)_6(3\text{-pic})_2(NO)]PF_6$ was prepared in phosphate buffer (pH 7.4) and 2 mL of it was irradiated under 660 nm light during 30 min in a fluorescence cuvette. A 100 μL aliquot was injected in NOA, under an $N_{2(g)}$ flow in order to detect the amount of NO released. Aiming to evaluate the NO release by chemical reduction stimulation, a 50 μL of the same solution (without exposure to light), was injected over 5 mL of a 45 mM solution of ascorbic acid under the $N_{2(g)}$ flow. NOA has the ability to measure concentrations in the range of 1 pM and has proven to be a tool widely used by researchers being cited in over 700 publications [48]. Due to the instability of the NO molecule, it reacts with ozone producing a quantity of light proportional to each reacted molecule. Through this reaction, the level of light produced is proportional to the NO concentration in the sample. Determination of NO moles is done based on the straight line obtained from the analytical curve (Supplementary information) of the device and the full area of the release curve.

4.3. Experimental procedure of aortic ring preparation

Male Wistar rats (180–200 g) were killed by decapitation in accordance with the Ethical Animal Committee, Ribeirão Preto Campus at the University of São Paulo, Brazil. The aorta was quickly removed, dissected free, and cut into 4 mm long rings. In order to avoid possible influence of endothelial factors, the endothelium was mechanically removed by gently rolling the lumen of the vessel on a thin wire. The aortic rings were placed between two stainless-steel stirrups and connected to an isometric force transducer (Letica Scientific Instruments) to measure tension in the vessels. The rings were placed in a 10 mL organ chamber containing Krebs solution with the following composition (mM): NaCl 130, KCl 4.7, KH_2PO_4 1.2, $MgSO_4$ 1.2, $NaHCO_3$ 14.9 glucose 5.5, $CaCl_2$ 1.6. The solution was maintained at pH 7.4 gassed with 95% O_2 and 5% CO_2 at 37 °C. The rings were initially stretched to a basal tension of 1.5 g (previously determined by length–tension relationship experiments), before allowing them to equilibrate for 60 min in the bath fluid, which was changed every 15–20 min. The aortic rings were stimulated continuously with 0.1 μM phenylephrine until reproducible contractile responses were obtained. The absence of endothelium was confirmed by the lack of relaxation response to 1 μM acetylcholine in aortic rings pre-contracted with 0.1 μM phenylephrine.

4.4. Relaxation induced by complex $[Ru_3O(CH_3COO)_6(3\text{-pic})_2(NO)]PF_6$ in pre-contracted arteries with phenylephrine

A 0.1 mM stock solution of **1** was prepared in DMSO. It was performed serial dilutions of the stock solutions in water. We have analyzed the maximal effect (ME) of the complex in concentration-effect curves constructed in rat aortic rings. To examine whether $[Ru_3O(CH_3COO)_6(3\text{-pic})_2(NO)]PF_6$ induces smooth muscle cell relaxation, aortic rings were pre-contracted with 0.1 μM phenylephrine and when the contraction had reached a plateau, the complex (0.1 nM–10 μM) was cumulatively added. The experiments were conducted in the presence or absence of visible light.

4.5. Statistical analysis

Data are expressed as mean ± SEM. In each set of experiments, n indicates the number of rats studied. Maximal effect (ME) was obtained from the concentration–response curves for $[Ru_3O(CH_3COO)_6(3\text{-pic})_2(NO)]^+$, being considered as the maximal amplitude response reached on those curves. The mean of individual values for each tissue was obtained using the GraphPad Prism version 3.0 (GraphPad Software Corporation San Diego, CA). Statistical significance was tested by one way ANOVA (post-test: Newman–Keuls) and Student's t test, and values of $P < 0.05$ were considered to be significant.

4.6. Molecular modeling

Geometries were obtained with RHF wavefunctions assuming singlet ground states with the PM3(tm) implementation of HYPERCHEM [60]. A conjugate gradient was used to achieve a 10^{-3} kcal mol^{-1} $Å^{-1}$ convergence for geometry. For the SCF calculations we used a 10^{-5} kcal mol^{-1} criterium for convergence of the wavefunction. Using these PM3(tm) geometries, molecular orbitals, vertical excitations and population analysis were obtained

with ZINDO/S wavefunctions obtained single excitations over an active space of 20 molecular orbitals (10 occupied plus 10 virtual).

Acknowledgments

The authors thank Professor Ana Maria da Costa Ferreira, form IQ – USP – São Paulo, for the acquisition of EPR spectra. We also thank Dr. Juliana Cristina Moraes Biazzotto and Clovis Junior for their collaboration to this work, Dr. José Carlos Tomaz for the acquisition of high resolution mass spectra, Prof. Dr. Roberto Santana da Silva for allowing the use of some equipments and the financial support from CAPES , CNPq and FAPESP agencies.

Appendix A. Supplementary material

Supplementary data associated with this article can be found, in the online version, at http://dx.doi.org/10.1016/j.ica.2015.01.038.

References

[1] R.G. de Lima, M. Gama, D. Bonaventura, A.C. Tedesco, R.F. Vianna, Inorg. Chim. Acta 358 (2005) 2643.
[2] M.G. Sauaia, R.G. de Lima, A.C. Tedesco, R.S. da Silva, Inorg. Chem. 44 (2005) 9946.
[3] R.D.L. Barreto, R.D. Correia, M.N. Muscará, Quim. Nova 28 (2005) 1046.
[4] E.C. Fornari, M.S.P. Marchesi, A.E.H. Machado, S. Nikolaou, Polyhedron 28 (2009) 1121.
[5] Z.N. da Rocha, R.G. de Lima, F.G. Doro, E. Tfouni, R.S. da Silva, Inorg. Chem. Commun. 11 (2008) 737.
[6] D.C.A.S. de Santana, T.T. Pupo, M.G. Sauaia, R.S. da Silva, R.F.V. Lopez, Int. J. Pharm. 391 (2010) 21.
[7] G. Stochel, A. Wanat, E. Kulis, Z. Stasicka, Coord. Chem. Rev. 171 (1998) 203.
[8] B.C.S. Allardyce, P.J. Dyson, Platinum Met. Rev. 45 (2001) 62.
[9] H.E. Toma, A.D.P. Alexiou, S. Dovidauskas, Eur. J. Inorg. Chem. 2002 (2002) 3010.
[10] H.E. Toma, A.D.P. Alexiou, A.L.B. Formiga, M. Nakamura, S. Dovidauskas, M.N. Eberlin, D.M. Tomazela, Inorg. Chim. Acta 358 (2005) 2891.
[11] R.C.L. Zampieri, G. Von Poelhsitz, A.A. Batista, O.R. Nascimento, J. Ellena, E.E. Castellano, J. Inorg. Biochem. 92 (2002) 82.
[12] S.A. Cicillini, A.C.L. Prazias, A.C. Tedesco, O.A. Serra, R.S. da Silva, Polyhedron 28 (2009) 2766.
[13] F. Marquele-Oliveira, D.C.D.A. Santana, S.F. Taveira, D.M. Vermeulen, A.R.M. de Oliveira, R.S. da Silva, R.F.V. Lopez, J. Pharm. Biomed. Anal. 53 (2010) 843.
[14] E. Tfouni, F.G. Doro, A.J. Gomes, R.S. Da Silva, G. Metzker, P.G.Z. Benini, D.W. Franco, Coord. Chem. Rev. 254 (2010) 355.
[15] M.G. Sauaia, F.D.S. Oliveira, R.G. De Lima, A.D.L. Cacciari, E. Tfouni, R.S. Da Silva, Inorg. Chem. Commun. 8 (2005) 347.
[16] R.G. de Lima, M.G. Sauaia, C. Ferezin, I.M. Pepe, N.M. José, L.M. Bendhack, Z.N. da Rocha, R.S. da Silva, Polyhedron 26 (2007) 4620.
[17] J.A. Baumann, D.J. Salmon, S.T. Wilson, T.J. Meyer, W.E. Hatfield, Inorg. Chem. 17 (1978) 3342.
[18] J.A. Baumann, S.T. Wilson, D.J. Salmon, P.L. Hood, T.J. Meyer, J. Am. Chem. Soc. 101 (1979) 2916.
[19] H.E. Toma, K. Araki, A.D.P. Alexiou, S. Nikolaou, S. Dovidauskas, Coord. Chem. Rev. 221 (2001) 187.
[20] M. Abe, A. Sato, T. Inomata, T. Kondo, K. Uosaki, Y. Sasaki, J. Chem. Soc., Dalton Trans. (2000) 2693.
[21] S.D. Glover, J.C. Goeltz, B.J. Lear, C.P. Kubiak, Coord. Chem. Rev. 254 (2010) 331.
[22] J. Qin, Y. Liao, X.-Y. Chen, C.-X. Qian, J.-L. Zuo, X.-Z. You, J. Organomet. Chem. 716 (2012) 275.
[23] A.D.P. Alexiou, S. Dovidauskas, H.E. Toma, Quim. Nova 23 (2000) 785.
[24] S. Nikolaou, A.L.B. Formiga, H.E. Toma, Inorg. Chem. Commun. 13 (2010) 1032.
[25] S.H. Toma, J.J. Santos, S. Nikolaou, K. Araki, H.E. Toma, Inorg. Chim. Acta 390 (2012) 148.
[26] S. Nikolaou, H.E. Toma, Eur. J. Inorg. Chem. 14 (2008) 2266.
[27] S. Ye, W. Zhou, M. Abe, T. Nishida, L. Cui, K. Uosaki, M. Osawa, Y. Sasaki, J. Am. Chem. Soc. 126 (2004) 7434.
[28] M. Abe, T. Michi, A. Sato, T. Kondo, W. Zhou, S. Ye, K. Uosaki, Y. Sasaki, Angew. Chem., Int. Ed. Engl. 42 (2003) 2912.
[29] Z.A. Carneiro, J.C. Biazzotto, A.D.P. Alexiou, S. Nikolaou, J. Inorg. Biochem 134 (2014) 36–38.
[30] F.A. Cotton, J.G. Norman, Inorg. Chim. Acta 6 (1972) 411.
[31] H.E. Toma, C.J. Cunha, C. Cipriano, Inorg. Chim. Acta 154 (1988) 63.
[32] M. Abe, Y. Sasaki, Y. Yamada, K. Tsukahara, S. Yano, T. Ito, Inorg. Chem. 34 (1995) 4490.
[33] J.C. Salsman, S. Ronco, C.H. Londergan, C.P. Kubiak, Inorg. Chem. 45 (2006) 547.
[34] M. Abe, Y. Sasaki, Y. Yamada, K. Tsukahara, S. Yano, T. Yamaguchi, M. Tominaga, I. Taniguchi, T. Ito, Inorg. Chem. 35 (1996) 6724.
[35] W. Zhou, Y. Zhang, M. Abe, K. Uosaki, M. Osawa, Y. Sasaki, S. Ye, Langmuir 24 (2008) 8027.
[36] T.S. Kurtikyan, V.A. Hayrapetyan, G.G. Martirosyan, R.K. Ghazaryan, A.V. Iretskii, H. Zhao, K. Pierloot, P.C. Ford, Chem. Commun. 48 (2012) 12088.
[37] B.L. Westcott, J.H. Enemark, Transition Metal Nitrosyls, John Wiley & Sons, Inc., 1999.
[38] P.C. Ford, B.K. Miranda, B. Lee, I. Lorkovic, S. Boggs, S. Kudo, L. Laverman, Coord. Chem. Rev. 171 (1998) 185.
[39] C.W. Bezerra, S.C. da Silva, M.T.P. Gambardella, R.H.A. Santos, L.M.A. Plicas, E. Tfouni, D.W. Franco, Inorg. Chem. 38 (1999) 5660.
[40] M.L. Bento, E. Tfouni, Inorg. Chem. 27 (1988) 3410.
[41] E. Tfouni, P.C. Ford, Inorg. Chem. 18 (1980) 72.
[42] E. Tfouni, M. Krieger, B.R. McGarvey, D.W. Franco, Coord. Chem. Rev. 236 (2003) 57.
[43] A.D.P. Alexiou, H.E. Toma, J. Chem. Res. (S) (1997) 338.
[44] S. Nikolaou, H.E. Toma, Polyhedron 20 (2001) 253.
[45] S. Nikolaou, M. Uemi, H.E. Toma, Spectrosc. Lett. 34 (2001) 267.
[46] I. Bertini, C. Luchinat, Coord. Chem. Rev. 150 (1996) 1.
[47] U. Schatzschneider, Eur. J. Inorg. Chem. 2010 (2010) 1451.
[48] <www.geinstruments.com/products-and-services/nitric-oxide-analyzer>, n.d. 2014, *134*, 36.
[49] M.A.W. Lawrence, P.T. Maragh, T.P. Dasgupta, Transition Met. Chem. 37 (2012) 505.
[50] S. Nikolaou, H.E. Toma, J. Chem. Soc., Dalton Trans. (2002) 352.
[51] T. Koshiyama, M. Shirai, T. Hikage, H. Tabe, K. Tanaka, S. Kitagawa, T. Ueno, Angew. Chem., Int. Ed. Engl. 50 (2011) 4849.
[52] A.J. Morris-Cohen, K.O. Aruda, A.M. Rasmussen, G. Canzi, T. Seideman, C.P. Kubiak, E.A. Weiss, Phys. Chem. Chem. Phys. 14 (2012) 13794.
[53] D. Bonaventura, Nitric Oxide 10 (2004) 83.
[54] M.S.P. Marchesi, S.A. Cicillini, A.C.L. Prazias, L.M. Bendhack, A.A. Batista, R.S. Silva, Transition Met. Chem. 37 (2012) 475.
[55] F.C. Munhoz, S.R. Potje, A.C. Pereira, M.G. Daruge, R.S. da Silva, L.M. Bendhack, C. Antoniali, Nitric Oxide 26 (2012) 111.
[56] G.J. Rodrigues, S.A. Cicillini, R.S. Silva, L.M. Bendhack, Nitric Oxide 25 (2011) 331.
[57] A. Spencer, G. Wilkinson, J. Chem. Soc., Dalton Trans. (1972) 1570.
[58] S. Kudo, J.L. Bourassa, S.E. Boggs, Y. Sato, P.C. Ford, Anal. Biochem. 247 (1997) 193.
[59] V. Mori, M. Bertotti, Analyst 125 (2000) 1629.
[60] "HyperChem Professional 8.0, Hypercube, Inc. 1115 NW 4th St. Gainesville, FL 32601, USA", n.d.